THE PRESENT STATUS OF KamLAND

Atsuto Suzuki
(for the KamLAND Collaboration)

Research Center for Neutrino Science, Tohoku University
Sendai, Miyagi 981-8578, Japan
E-mail: suzukia@awa.tohoku.ac.jp

Abstract

Almost two years has passed since the KamLAND project started. The present status of the detector construction and R&D work is presented. The KamLAND direct test of the large mixing angle solution to the solar neutrino problem is getting quite important from oscillation analyses of the current solar neutrino data.

1 Introduction

KamLAND, a general purpose detector with 1,000-ton liquid scintillator for exploring the lower energy neutrino and anti-neutrino physics, has been under construction since 1998. One of primary targets in the KamLAND physics is to search for neutrino oscillations with reactor anti-neutrinos. The large mixing angle solution, (Δm^2, $\sin^2 2\theta$) = ($\sim 10^{-5}, > 0.6$) is verified or excluded thanks to a 170 km long flight distance and a 1 kton large target mass.We also aim to detect the ^{8}B and ^{7}Be solar neutrinos after getteing ultra pure liquid scintillartor by recirculating the liquid scintillator through purification. The KamLAND detector designing work focuses on giviing potentials for both physics researches. The data-taking is planed to start in 2001.

2 KamLAND Construction

The KamLAND detector is comstructed at the old Kamiokande site, dismantling the 3,000-ton water Cerenkov detector. The rock-overburden is 2,700 m.w.e. on average and the cosmic-ray muon rate is expected to be about 0.3 Hz inside the detector. The detector structure consists of 3 layers as illustrated in Fig. 1. The outer layer is the 6,200-m^3 water pool, which is used as the water Cerenkov anti-counter. The middle is the 3,000-m^3 stainless steel spherical tank. Paraffin oil is filled in this tank. The inner most structure is the 1,200-m^3 plastic balloon filled with liquid scintillator. The KamLAND detector construction in the mine side began in April 1998.

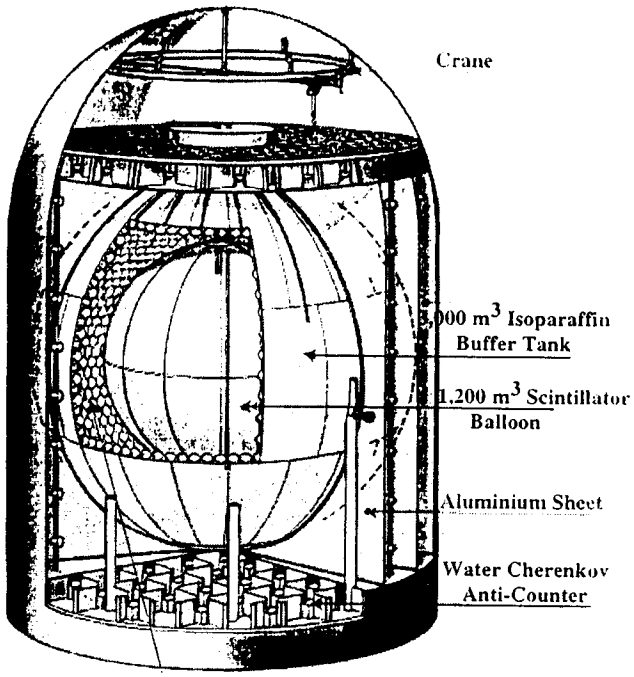

Figure 1: Schematic view of the KamLAND detector.

2.1 Underground Laboratory

To begin with, 1,000 20-inch photo-multiplier tubes (PMTs) were dismantled from the Kamiokande 3,000-ton water Cerenkov detector. These PMTs are reused for the KamLAND water Cerenkov anti-counter after reinforcing a waterproof structure. Then the mine tunnel reaching from the Super-Kamiokande area was enlarged to be 4.3 m wide and 3.8 m high. This new tunnel enables us to access to the KamLAND underground laboratory from the mine entrance by using a large car. Scrapping the Kamiokande water tank took 3 months from last October. In January 1999 all the equipment of Kamiokande was removed from the detector cavity. The floor level of this cavity was then lowered by 4 m, which gives the KamLAND cavity with 20 m-diameter $\times$ 20 m height. A water pool construction by lining polyurethane resins on the cavity rock surface was finished until the end of March 1999. Fig. 2 shows the 6,200 m^3 water pool viewed form the bottom floor. A set of compensating coils is installed next year on the top, bottom and wall surfaces of this pool, which insures that the Earth's magnetic field is reduced down to less than 50 mGauss inside the 3,000 m^3 stainless steel spherical tank. Electric high voltage (3 kV) power lines from the mine power station were renewed, and preparing the main power station and local stations in the underground laboratory was also completed until March 1999. The Rn free-air ventilation system, fire proof shutters and monitoring-alarming system of fire, heat and organic gases are also installed until March 2000.

Figure 2: Anti-counter water pool.

2.2 3,000 m^3 Buffer Oil Tank and 17-inch PMT

A stainless steel spherical tank with an 18-m diameter is solidly mounted inside the water pool. A construction of this tank will start in August 1999. Contamination of radioactivity in welding materials and stainless steel tank materials has been measured to select low radioactive detector materials, and at the same time how to remove welding mists on construction has been considered. The 4-m diameter and 2.5-m height nozzle is set on the top of the tank, where the recirculation pipes of the liquid scintillator and buffer oil, the balloon chimney and the chimney for guiding the calibration tools are supported through this nozzle.

Buffer oil, the mixture of isoparaffin and normal paraffin with an equal weight is filled inside the tank in order to give a little density difference from the liquid scintillator. An attenuation length of the paraffin oil for 400-nm light is found to be 30 m. 1,280 newly developed 17-inch PMTs are uniformly mounted on the inner surface of the spherical tank, giving about 22 % photosensitive coverage. We also have the plan to mount additional 642 17-inch PMTs by the US proposal. A regular PMT production started last year. About 1,000 PMTs have been already delivered to Tohoku University, where detailed performance measurements, assembling the PMT support structures and cleaning all parts attached to PMT are carried out. Characteristics of the new PMT obtained at 10^7 gain are compared with those of the 20-inch Super-Kamiokande PMTs in Fig. 3. Significant improvements can be seen in the transit-time-spread (TTS) of 3 ns at FWHM and the output pulse-height shape with the peak to valley ratio of 3.3 both for single photo-electron (p.e.) diffused illumination. A relatively high rate (25 kHz on average) of the dark pulse obtained with the

0.25 p.e. pulse-height threshold, can be seen in this figure. An active photo-cathode due to short duration after production causes such a high noise rate. However by having left them in a dark room for half a year, this rate calms down to 5 kHz on average at the room temperature. The 17-inch PMT has the same shape and size as those of the 20-inch PMT, but photo-cathode sensitivity is limited only inside the central 17 inches of the front face. Therefore a black acrylic cap is attached to mask the outer area of photo-cathode. Inside the tank the spaces between neighboring PMTs are blind by connecting black sheets with the black acrylic caps. A total of 120 rhombus shape acrylic plates with a thickness of 3 mm and a side length of about 2.7 m are placed in front of all the PMT plane. Thus the buffer oil space is divided into two layers. This acrylic wall makes a key role to protect the Rn diffusion toward the liquid scintillator balloon, where Rn emanates from the PMT glass, the stainless steel tank and unexpected dusts remained on all materials inside the tank. The construction of the tank, PMT support structure and acrylic structure will be finished until the end of March 2000.

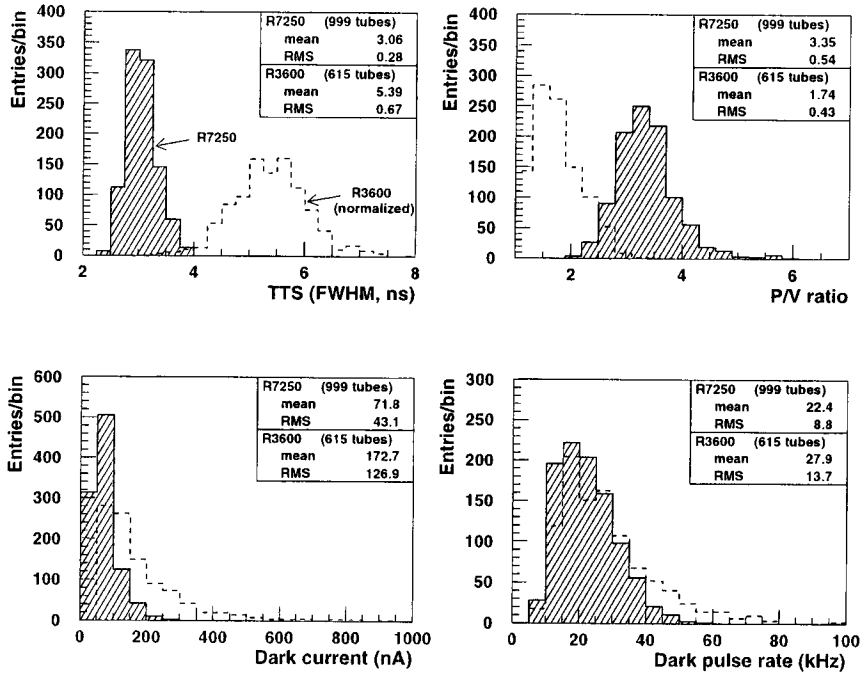

Figure 3: Properties of the 999 KamLAND 17-inch tubes (shaded histograms) and the fast 615 20-inch Super-Kamiokande tubes (dashed histograms).

2.3 1,200 m^3 Plastic Balloon and Liquid Scintillator

The plastic balloon with a diameter of 13 m contains 1,000-ton liquid scintillator in a spherical shape. Since the density of the KamLAND liquid scintillator is adjusted to

be 1 % heavier than that of the buffer oil, the balloon is wrapped by a plastic lope net and suspended by tens of lopes from the tank nozzle (see Fig. 4). The sandwiched film of EVOH (polyvinyl alcohol)/nylon/EVOH was developed as the KamLAND balloon material. EVOH with low permeability of Rn ($< 10^{-10}$ μm/s) prevents Rn-invading into the liquid scintillator from outside the balloon by two EVOH films and from radio impurities in nylon by one film. The transparency of the 75 μm sandwiched film is found to be about 96 % for 400-nm light. Producing much thicker films is now being developed. The balloon and its support structure will be prepared until March 2000.

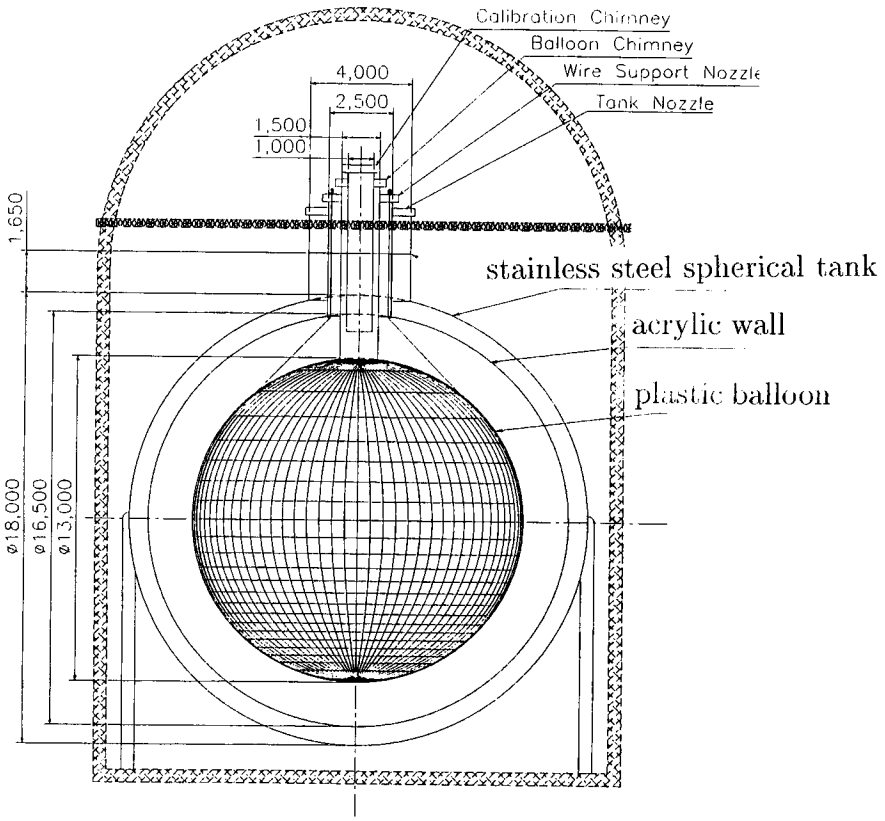

Figure 4: Design of the KamLAND detector.

The KamLAND liquid scintillator cocktail is composed of normal paraffin (80 %), pseudocumene (1,2,4-Trimethylbenzene) (20 %) and PPO (Diphenyloxazole) (2g/l). The light output of this scintillator is equal to about 50 % of Anthracene. The light attenuation length is 10 m for 400 nm light and 20 m for 450 nm light. The light output produced by cosmic-rays was measured, using the 6.5 m long pipe (the same length as the balloon radius) filled with scintillator. The result gives 160 p.e./MeV light output expected in the KamLAND detector, combining the light response properties of the balloon, buffer oil and 17-inch PMT. Pulse-shape discrimination between scintillation produced by neutrons and γs is crucial to suppress backgrounds from radioactive decays. We obtained 90 % of the neutron rejection efficiency among γ-like

signals, using a small size detector. Further study is being carried out at the Test Bench Facility, in which the liquid scintillator balloon with a diameter of 90 cm is equipped. A quenching factor of the scintillation for 7.7 MeV α particles is measured to be about 14. Filling the liquid scintillator into the balloon is scheduled from August 2000.

Radioactivity in the liquid scintillator is a serious background source for the KamLAND physics. Contamination of U, Th and K in the liquid scintillator without purification is measured to be 2×10^{-13} g/g, $< 5 \times 10^{-12}$ g/g and 7×10^{-11} g/g, respectively. After purifying through the water-extraction method, the contents of U, Th and K are reduced to be $< 10^{-13}$ g/g for U/TH and $< 10^{-12}$ g/g for K, where these limits come from the present measuring sensitivity in using a ICP-mass separator. The Monte Carlo study tells that the above radio-impurity levels of the liquid scintillator make it possible to give meaningful results on the reactor neutrino oscillation searches. But 2 order of magnitude improvement for removing U/Th and 1 order of magnitude for K are necessary to detect the ^{7}Be solar neutrinos.

The 2 m^3 liquid scintillator Test Bench Facility was constructed in Tohoku University. Various tests on the balloon materials and its support structure, the liquid scintillator performance, the 17-inch PMT performance, the purification techniques, and on-line data taking programs are being carried out (see Fig. 5).

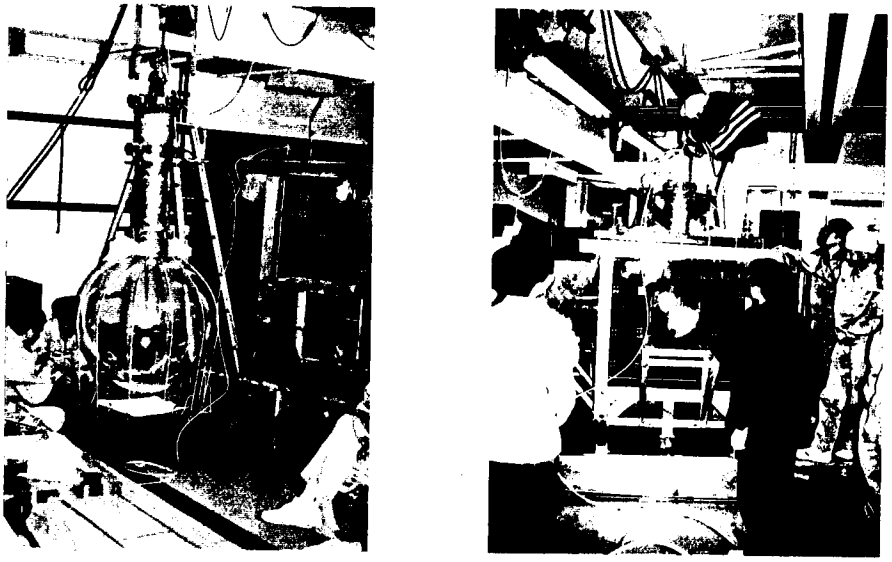

Figure 5: Working at Test Bench Facility.

3 Long Baseline Neutrino Oscillation Search

Neutrino oscillation searches with a 170 km long baseline is carried out in KamLAND, utilizing commercial nuclear power plant reactors. The event rate/year/1 kton in KamLAND is plotted in Fig. 6as a function of the distance from Kamioka . One can

find that 85 % of total events come from reactors with 140-200 km apart. Thus it is a strong feature that this experiment is almost equivalent to use one big reactor with 67 GWatt thermal at the maximum power at the distance of (175 ± 35) km away from the detector.

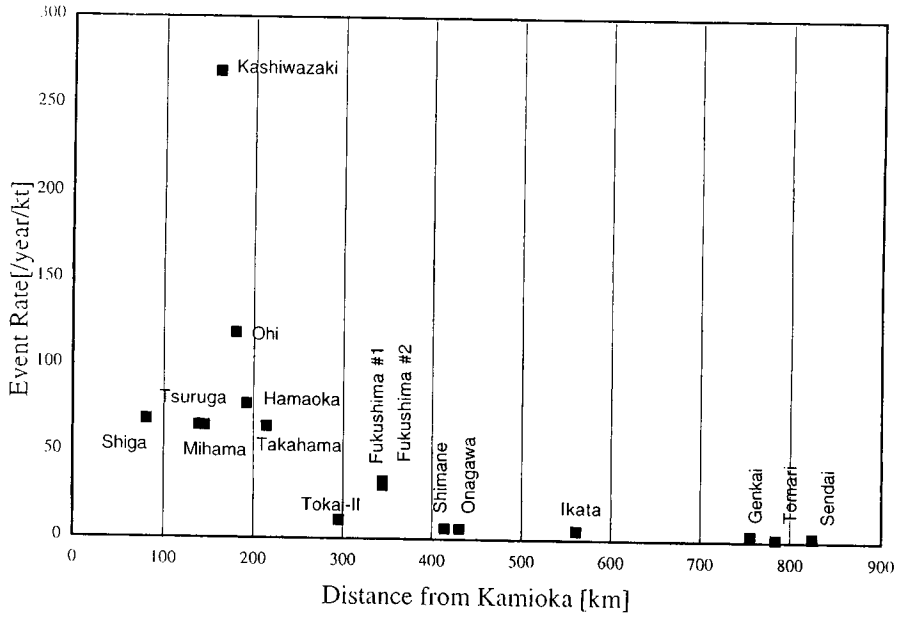

Figure 6: Expected event rate in units of yr^{-1} kton $^{-1}$ from available power plant reactors as a function of the distance from Kamioka.

Reactor anti-neutrinos with energies above 1.8 MeV are measured by detecting the inverse β-decay events, $\bar{\nu}_e p \rightarrow e^+ n$. The timing coincidence, position correlation and energy constraint between a prompt e^+ signal and a delayed 2.2 MeV γ produced by a thermal neutron capture on a free proton make it possible to identify the inverse β-decay events among a large amount of background. About 450 inverse β-decay events are expected for one year operation with the 600 ton fiducial mass, assuming that an annual average of reactor operation is 80 % of the maximum. On the other hand the number of corresponding background events is 7.5, where radio-impurity in the liquid scintillator of 10^{-14} g/g for U/Th, 10^{-12} g/g for K and 0.5 mBq/m^3 is assumed, and the data of γ-ray measurements inside the detector cavity is used. Fig. 7 shows the expected energy spectrum of positrons produced by reactor anti-neutrinos together with that of background events. Background events distribute in the energy less than 3 MeV. 7 events come from the liquid scintillator and 0.5 events from the surrounding rocks.

The excluded region in the Δm^2-sin$^2 2\theta$ plane for $\nu_e - \nu_\mu$ oscillations is obtained from the total detected number of events. Fig. 8 depicts the 90 % C.L. contour for the KamLAND 3-year operation together with the results of other reactor experiments. KamLAND improves more than 2 order of magnitude in the Δm^2 sensitivity, com-

332334

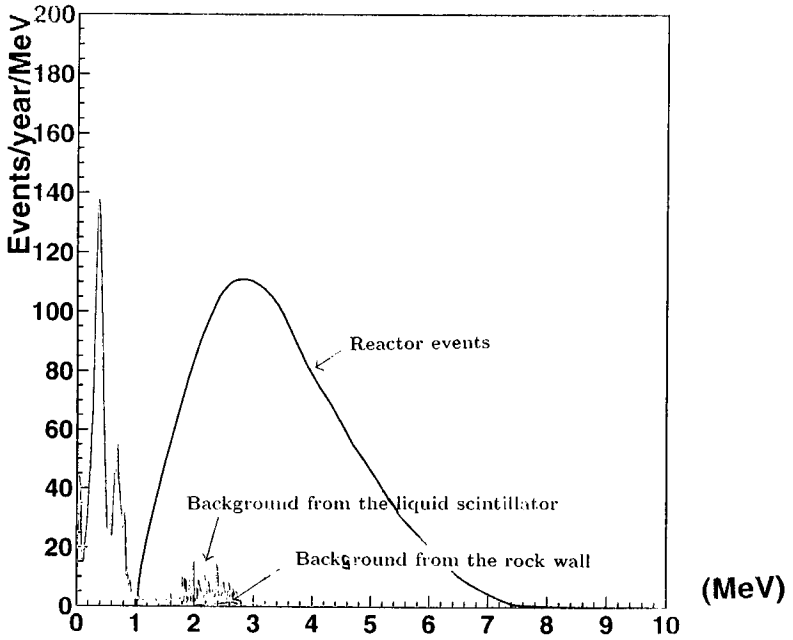

Figure 7: Expected visible positron energy spectra induced by reactor anti-neutrinos and come from correlated background events.

pared with CHOOZ and Palo Verde. The most interesting potential in KamLAND is that the large mixing angle (LMA) solution interpreting the solar neutrino deficit can be examined by direct measurements with an artificial neutrino source.

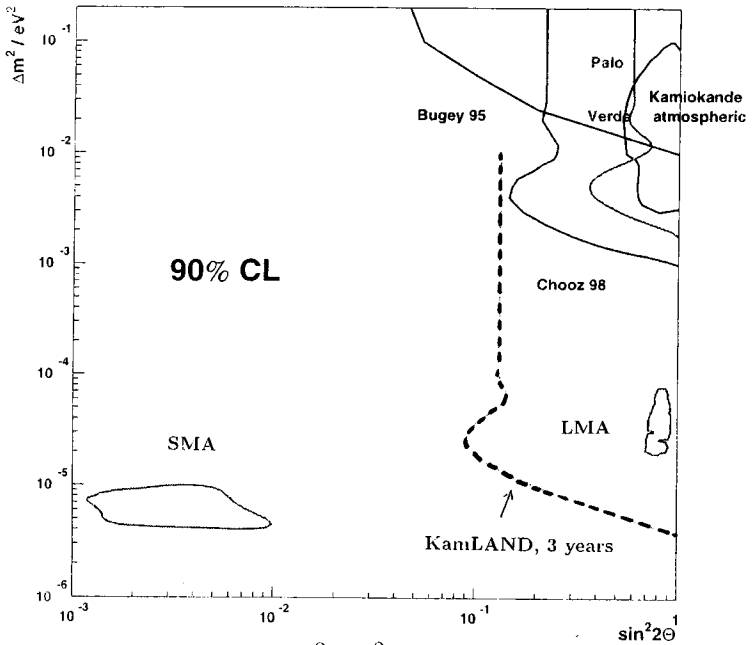

Figure 8: Excluded regions in the Δm^2-$\sin^2 2\theta$ plane for $\nu_e - \nu_\mu$ oscillations in the current and future experiments together with the large mixing angle (LMA) and small mixing angle (SMA) solutions to the solar neutrino problem.

In the inverse β-decay process the positron energy determines the incident anti-neutrino energy by $E_{e+} = E_{\bar{\nu}_e} - \Delta m$, where $\Delta m = 1.293$ MeV is the neuron-proton mass difference. Therefore the positron energy distribution is directly modified by neutrino oscillations, depending on oscillation parameters. Fig. 9(a) shows the expected visible positron energy spectra for different oscillation parameters. Using a deviation from the energy spectrum without oscillations provides the unique oscillation analysis free from the absolute anti-neutrino flux. Fig. 9(b) is the plot of the positron energy spectra with oscillations normalized by that without oscillations. The most probable oscillation parameters to explain all available solar neutrino data, assuming the absolute hep neutrino flux to be free, are obtained to be $(2.5 \times 10^{-5}, 0.79)$ of $(\Delta m^2\text{-}\sin^2 2\theta)$ [1]. One can find that this parameter set gives a large deviation in the energy spectrum as shown in Fig. 9(b).

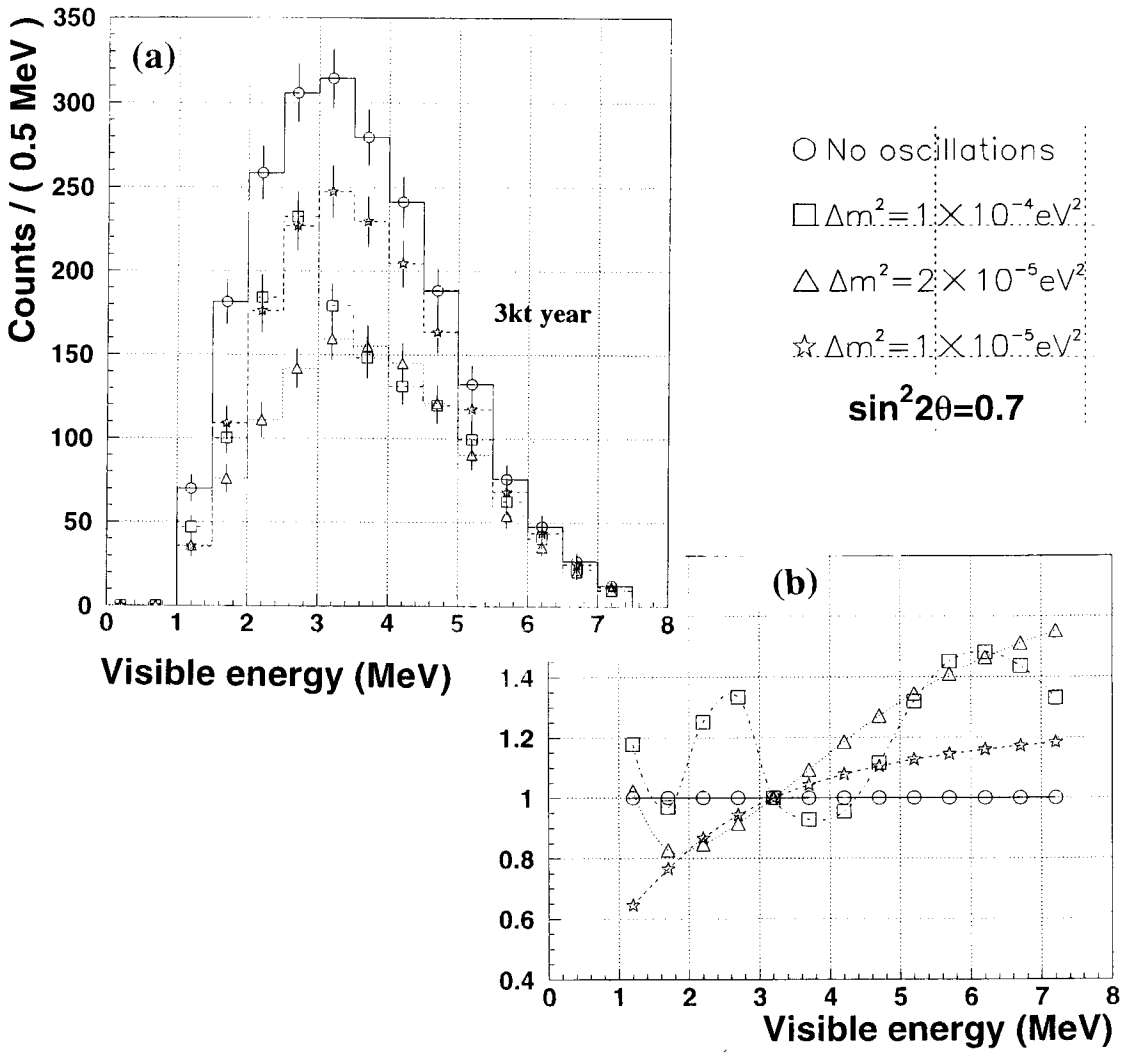

Figure 9: (a) The visible positron energy spectrum from reactor neutrinos expected in KamLAND for different oscillation parameter sets. (b) The ratio of the spectrum with oscillations to that without oscillations normalized at 3 MeV.

Annual operation time of the Japanese commercial power plant reactors is restricted by the legal obligation to have 3 months shutdown for maintenance. The shutdown period concentrates on spring or fall, because of not much demand for electric power. Fig. 10 shows the variation of the electric power flux at Kamioka from the Japanese reactors for past 5 years. 30 % variations can be seen in this figure.

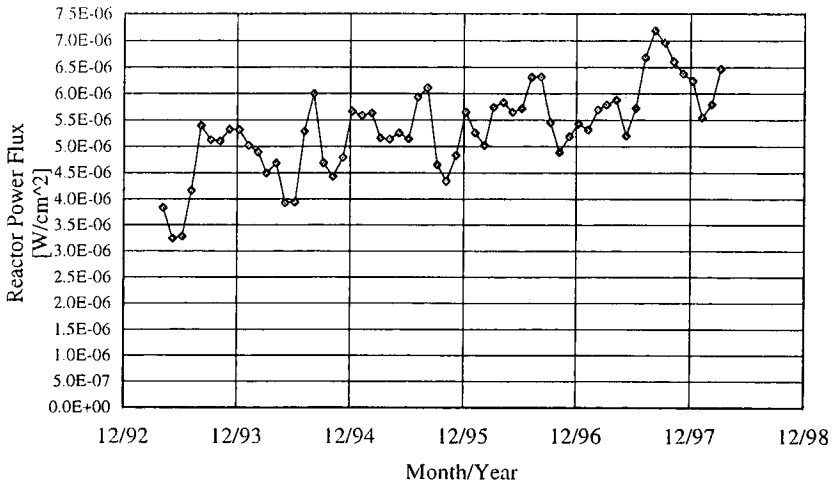

Figure 10: Monthly reactor power flux variation at Kamioka from available reactors for past 5 years.

This annual variation of the reactor power flux also provides the oscillation analysis free from the absolute neutrino flux. Assuming that the same flux variation as in 1997 continues in future, the 5 year KamLAND operation observes the monthly event rate change depending on the reactor power flux. Fig. 11 shows the plot of the event rate vs. the power flux without oscillations and with the LMA oscillation of Δm^2-$\sin^2 2\theta = (2.5 \times 10^{-5}, 0.79)$. The LMA solution gives the apparent slope change as shown in Fig. 11.

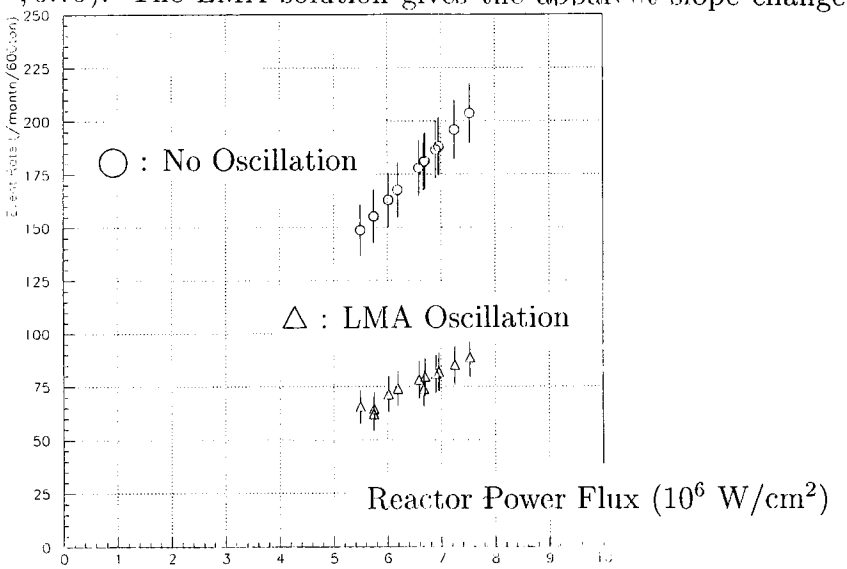

Figure 11: Seasonal event rate variation obtained by the 1997 data with 5 year statistics.

385337

In the neutrino oscillation search with reactor anti-neutrinos, the terrestrial anti-neutrinos would be a serious background source. 40~150 events are expected in one year with 1 kton target mass, depending on geophysical models [2]. Since the maximum visible positron energy produced by terrestrial neutrinos is 2.5 MeV, it is conservative to use positron events with the energy above 3.5 MeV in the reactor neutrino oscillation analysis. Fig. 12 shows the 90 % C.L. sensitivity of reactor neutrino oscillation searches in KamLAND, using positron events with the energy above 3.5 MeV. Here the solid curve represents the excluded region given by the total detected number of events for one year operation. The dotted curve is given by the spectrum shape change for 3 year operation. The dashed curve is given by the annual flux variation for 3 year operation. Three different curves are possible to cover the LMA solution parameters.

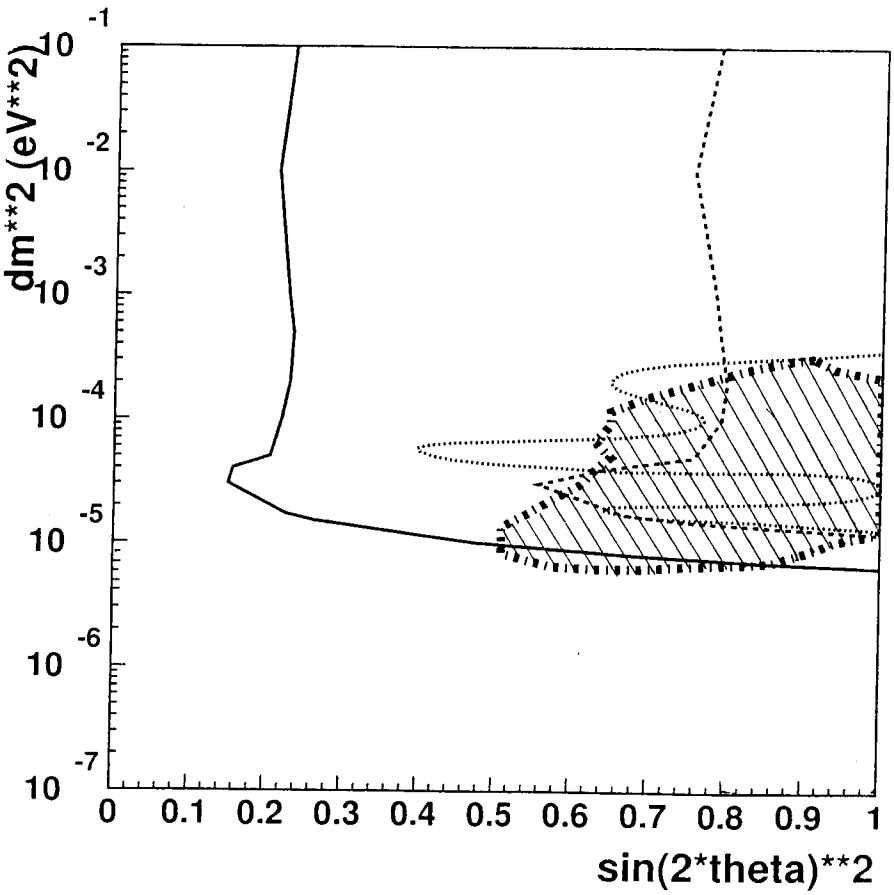

Figure 12: Parameter constraints at 90 % C.L. on $\nu_e \rightarrow \nu_x$ oscillations obtained by using events with the energy above 3.5 MeV. The sloid curve is derived from the number of detected events, the dotted curve from the spectrum change and the dashed curve from the annual flux variation. The shaded region is the LMA solution.

336 33

4 Conclusion

The KamLAND detector construction goes into the most productive stage this year. Constructing the 3,000 m^3 stainless steel tank, 1,200 m^3 plastic balloon, and installing the 17-inch PMTs inside the tank will be done within a year or so. Then the liquid scintillator mixing and filling into the ballon will start next summer. And we plan to begin the data-taking in 2001.

5 Acknowledge

We would like to thank for discussions to the KamLAND collaborators: P. Alivisatos, S. Berridge, N. Bokor, C. Britton, W. Bryan, W. Bugg, J. Busenitz, R.N. Cahn, Y.D. Chan, X. Chen, T. Chikamatsu, F.H. Cocks, H. Cohn, L. DeBraeckeleer, B.Dieterle, Yu. Efremenko, S. Enomoto, S. Frank, S.J. Freedman, B.K. Fujikawa, K. Furuno, H. Gando, C.R. Gould, G. Gratta, H. Hanada, E. Hart, S. Hatakeyama, M. Higuchi, G. Horton-Smith, C.R. Howell, H. Ikeda, K. Inoue, K. Ishihara, T. Itoh, T. Iwamoto, T. Kawaguchi, Yu. Kamyshkov, B.-K. Kim, H. Kinoshita, M. Koga, J. Kornis, C.E. Lane, K.B. Lee, K.T. Lesko, H.L. Liew, K.-B. Luk, R.D. MaKeown, L. Miller, T. Mitsui, H. Murayama, M. Nakajima, T. Nakajima, K. Nakamura, A. Nemeth, V. Novikov, D.R. Nygren, H. Ogawa, C.E. Okada, K. Oki, H. Ohtani, P. Pacher, A. Pipke, A.W. Poon, S. Riley, N. Sleep, J. Shirai, R. Steinberg, H.M. Steiner, F. Suekane, R.C. Svoboda, K. Tagashira, O. Tajima, T. Takayama, K. Tamae, H. Tanaka, T. Taniguchi, W. Tornow, D. Tracy, P. Vogel, Y-F. Wang, H. Watanabe, A. Witenberg, J. Wolf and J. Wolker.

References

[1] Super-Kamiokande, private communication.

[2] R.S. Raghavan, S. Schoenert, S. Enomoto, J. Shirai, F. Suekane and A. Suzuki, *Phys. Rev. Lett.* **80** (1998) 635.